

# Origin and orientation of microporosity in eclogites of different microstructure studied by ultrasound and microfabric analysis

**Matěj Machek<sup>a</sup>, Petr Špaček<sup>a,b</sup>, Stanislav Ulrich<sup>a,c</sup>, Florian Heidelberg<sup>d</sup>**

<sup>a</sup> Geophysical Institute, Czech Academy of Sciences, Prague, Czech Republic

<sup>b</sup> Institute of Earth Physics, Masaryk. Univ., Brno, Czech Republic

<sup>c</sup> Institute of Petrology and Structural Geology, Fac. Nat. Sci., Prague, Czech Republic

<sup>d</sup> Univ Bayreuth, Bayer Geo Inst, Bayreuth, Germany

***published in Engineering Geology 89 (2007) 266–277***

This work contributes to the experimental investigations of the origin and 3-D orientation of micropores in low porosity crystalline rocks. The origin and spatial orientation of microporosity in two eclogites with different microstructure were studied by 1) quantitative and qualitative microstructural analysis of grains and grain boundaries, 2) measurement of lattice preferred orientation using the SEM-EBSD method and 3) experimental measurement of velocity of elastic P-waves in spherical samples in 132 directions under confining pressures up to 400MPa. Results show good correlation between the elastic properties and the orientation of grain boundaries and cleavage planes in clinopyroxene. The magnitude and anisotropy of velocity change with pressure shows that microporosity in the fine-grained sample is relatively large and strongly preferentially oriented, whereas it is significantly lower and less preferentially oriented in the coarse-grained sample. Seeing that the lattice preferred orientation of clinopyroxene is similar in both samples we can deduce from velocity changes that the grain size of the rock forming minerals controls the amount of microporosity. Also, the orientation of microporosity depends mostly on preferred orientation of grain boundaries and somewhat less on the orientation of cleavage planes. Grain boundaries are therefore the most important contributors to the bulk microporosity in the studied rocks.

## 1 Introduction

Crystalline rocks of metamorphic or igneous origin are usually of very low porosity (below 2%), and hence they are suitable as a natural barrier for dangerous waste stored in underground repositories. The waste repository site is usually situated in a rock mass of low porosity with minimum content of macroscopic fractures, which are most

efficient for contaminant migration. In such places, spatial distribution and origin of microporosity is of great interest in order to describe physical pathways for fluids and if possible, to define the depth level, below which the majority of micropores is closed.

In general, microporosity follows grain boundaries, cleavage planes of rock forming minerals and inter- or intra-granular microfractures of different length that can be either sealed or open (e.g. Babuška and Pros, 1984; Siegesmund and Vollbrecht, 1991; Schild et al., 2001; Takeshita and Yagi, 2001; Akesson et al., 2004). Orientation and anisotropy of micropores may be used to estimate permeability anisotropy, deformational history or direction-depedendent technical parameters of the rocks. However, there are only a limited number of methods for the determination of oriented microporosity. Traditionally, it is carried out with U-stage measurements in three orthogonal sections and then combined to equal area pole diagram (e.g. Siegesmund et. al. 1991). An orientation of microcracks, cleavages and individual grain boundary types between constituent minerals are evaluated using back-scattered electron (BSE) images (e.g. Kanaori et al., 1991) or confocal scanning laser microscopy (Menendez et.al., 2001).

A number of laboratory investigations of rock samples have demonstrated that microcracks significantly decrease elastic wave velocities (e.g. Birch, 1961; Brace, 1965; Babuška and Pros, 1984) and that with increasing depth (lithostatic pressure), the majority of microcracks progressively closes down, while the velocity of elastic waves increases (e.g. Birch, 1961). Oriented systems of porosity may cause velocity anisotropy even if the matrix of the rock is almost isotropic (Babuška et al., 1977). If measurements have been carried out on a spherical sample in many directions, the difference between P-wave velocities measured at atmospheric pressure and at a higher hydrostatic pressure is a useful tool for the visualization of microporosity (velocity difference -  $\Delta V_p$ ) in a stereodiagram (Babuška and Pros, 1984; Siegesmund et al., 1993). Babuška and Pros (1984) correlated opening of major cleavage planes and cracks as a function of confining pressure in the case of granodiorite and quartzite. In case of granodiorite, preferred orientation of major cleavage planes in biotite and amphibole correlates well with the areas of the biggest difference in P-wave velocities, although these minerals represent only 9 % of the volume, and they remain open up to 300 MPa confining pressure. On the contrary, preferentially oriented irregular microcracks in almost monomineralic quartzite have a smaller effect on the velocity anisotropy and they are closed already at about 100MPa. The flat cleavage cracks and their orientation have the strongest influence on elastic wave velocities and their anisotropy at atmospheric and low hydrostatic pressures (Babuška and Pros, 1984). Siegesmund et. al. (1993) investigated the influence of rock fabric on the spatial distribution of P-wave velocities in orthogneisses. They correlated directions of high P-wave velocity differences at low confining pressures with directions of minimum values of P-wave velocities. Cleavage cracks in biotite and grain boundary cracks parallel to foliation have the main influence on elastic wave velocity in orthogneiss and its anisotropy at low pressures.

In this work, we examine origin and orientation of microporosity in two eclogites of similar lattice preferred orientation (LPO) of clinopyroxene but different grain size and microstructure using 1) qualitative and quantitative microstructural analysis of grains and grain boundaries orientation in three thin sections that are oriented parallel to XZ, XY and YZ planes of finite strain ellipsoid, 2) measurement of lattice preferred orientation using the electron backscattering diffraction (EBSD) method and 3) experimental measurement of the velocity of acoustic P-waves in spherical samples in 132 directions under confining pressures up to 400MPa. Two samples of eclogite (JK1b and SNW3) presented in this work provide different microstructural characteristics that refer to

different metamorphic and deformational evolution (Fig.1). The first sample (JK1b) is a dynamically recrystallized fine-grained crustal eclogite. The second sample (SNW3) belongs to the population of coarse-grained mantle eclogite xenoliths. We choose eclogites as a simple bi-mineral rock type composed of omphacite and garnet as cleavage-bearing anisotropic and cleavage-free isotropic minerals, respectively.

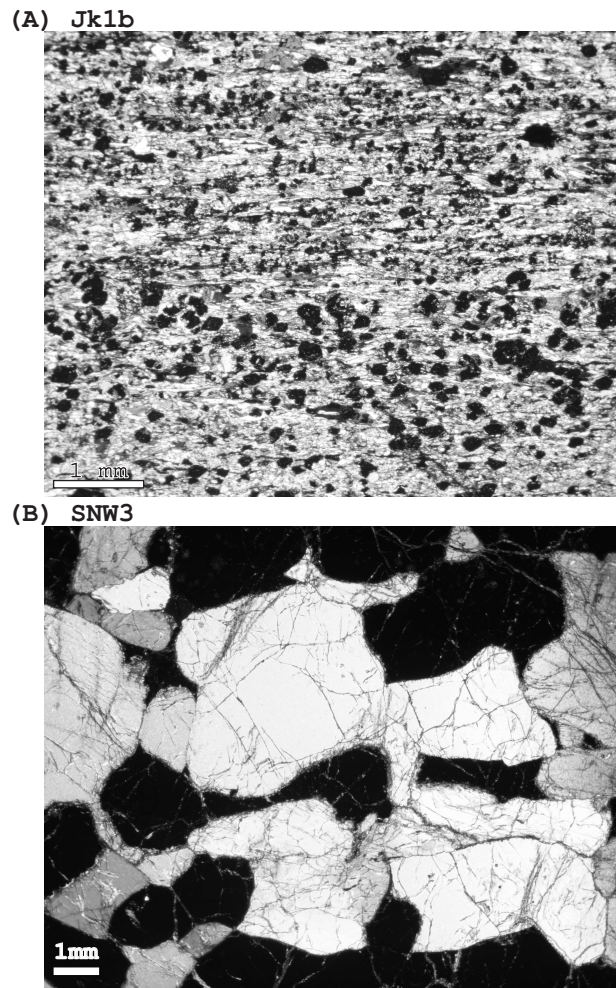


**Figure 1.** Micrographs of thin sections illustrating the microstructure of a) sample JK1b and b) sample SNW3. Thin sections were prepared from spherical samples after experimental measurement of seismic velocities parallel to lineation and perpendicular to foliation in order to carry out quantitative microstructural and SEM-EBSD analyses. The majority of visible cracks in the sample SNW3 developed during the decrease of confining pressure at P-wave velocity measurements and also during thin section preparation.

## 2 Microstructural and grain boundary orientation analyses

A quantitative microstructural analysis of grain boundaries was carried out in ESRI ArcView© 3.3 GIS environment. Grains were manually traced from micrographs obtained from three thin sections cut parallel to XZ, YZ and XY planes of finite strain ellipsoid (Fig. 2). The map of grain boundaries was generated using ArcView extension Poly (Lexa et al., 2005). The resulting polygons have been treated by MATLAB™ PolyLX Toolbox (Lexa et al., 2005) and used for quantitative microstructural analysis. Average

**Table 1** Summary of microstructural analysis of studied samples

	Phase	% of volume fraction	Mean Feret diameter	Mean axial ratio		
				xz	xy	yz
JK1B	cpx	53.3	41.13 [ $\mu\text{m}$ ]	2.46	2.39	1.74
	grt	30	87.05 [ $\mu\text{m}$ ]	1.42	1.44	1.30
	amp	7.58	118.59 [ $\mu\text{m}$ ]	1.52	2.47	1.84
	ru	3.52	29.21 [ $\mu\text{m}$ ]	2.46	2.16	1.74
	q	2.9	65.30 [ $\mu\text{m}$ ]	1.64	2.20	1.54
	par	2.27	93.82 [ $\mu\text{m}$ ]	x	x	2.45
	zo	0.44	48.70 [ $\mu\text{m}$ ]	1.72	x	x
SNW3	cpx	55.97	1.31 [mm]	1.96	1.78	1.75
	grt	44.03	2.20 [mm]	2.05	1.80	1.97

Modal mineralogies (%), mean Feret diameter ( $\mu\text{m}$  for sample JK1b and mm for sample SNW3), mean axial ratio. Axial ratio data are presented separately for sections parallel to XZ, YZ and XY planes of finite strain ellipsoid. cpx-clinopyroxene, grt-garnet, amp-amphibole, ru-rutile, q -quartz, par-paragonite, zo-zoisite.

grain size is given as Feret diameter ( $F = 2\sqrt{(A/\pi)}$ , where A is area of grain). Grain boundary preferred orientation was determined using the moment of inertia ellipse fitting and eigen analysis of bulk orientation tensor technique and its degree is expressed as eigenvalue ratio of weighted orientation tensor of grain boundaries. Grain boundary orientation is presented in rose diagrams corresponding to circular histograms of grain boundaries frequency (Fig. 2). All data obtained from grains and grain boundaries orientation analyses are summarized in Table 1 and 2.

## 2.1 Fine-grained eclogite (JK1b)

The sample of fine-grained eclogite comes from a lens of eclogite emplaced in anatectic orthogneiss of the Czech part of the Krušné hory Mts., Bohemian Massif. An equilibration temperature of 600 - 650° and peak metamorphic pressure of 2.6 GPa were estimated for this eclogite (Klápová et al., 1998). The studied sample is a fine-grained mylonite with well developed macroscopic foliation and lineation defined by elongated clinopyroxene grains. The rock consists of 53.3% clinopyroxene, 30% garnet, 7.6% amphibole, 3.5% rutile, 2.9% quartz, 2.3% white mica (paragonite) and 0.4% zoisite (Table II.1). Clinopyroxene is dynamically recrystallized to an elongated fine grain size ranging between 3  $\mu\text{m}$  and 265  $\mu\text{m}$  with a mean Feret diameter of 41  $\mu\text{m}$ . Garnet grains have idiomorphic shapes with size ranging between 7  $\mu\text{m}$  to 386  $\mu\text{m}$  with a mean Feret diameter of 87  $\mu\text{m}$ . The mean axial ratio of clinopyroxene and garnet grains ranges from 1.74 in YZ section to 2.46 in XZ section and from 1.30 in YZ section to 1.44 in XY section respectively (Table II.1). Orientation of grain boundaries is influenced mostly by clinopyroxene, which is the most abundant mineral. Eigenvalue ratios show a constrictional fabric of grain boundaries with strong preferred orientation in XZ (1.76) and XY (1.69) sections, while in YZ section the eigenvalue ratio is significantly lower (1.12). Thereby the grain boundaries form a constrictional fabric almost parallel to the direction of macroscopic lineation (deviating 10° from it).

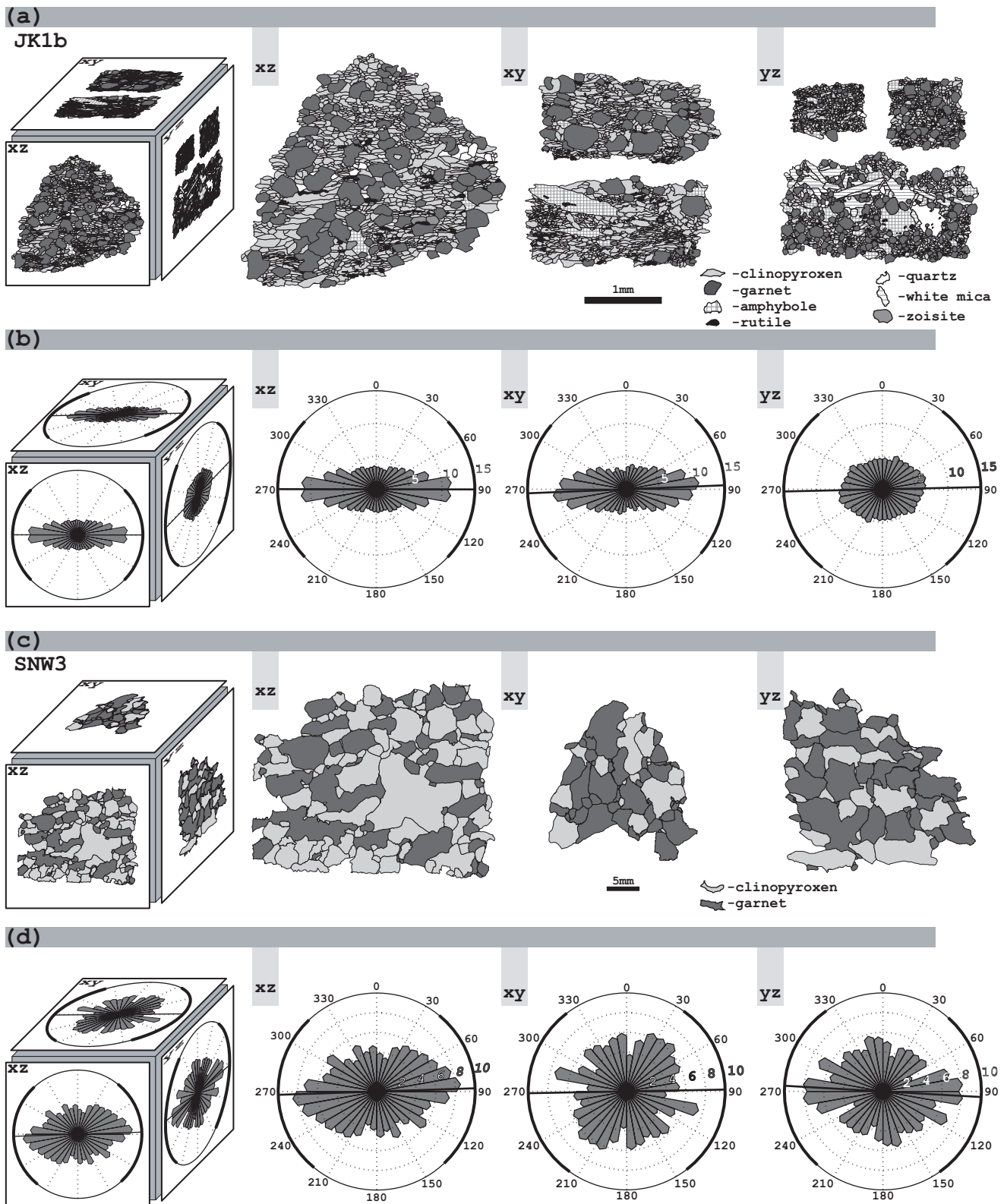


**Figure 2.** Digitized microstructure and rose diagrams of grain boundary orientation of all phases of sample JK1b (a, b) and sample SNW3 (c, d) obtained from sections parallel to XZ, YZ and XY planes of finite strain ellipsoid. Therefore foliation is horizontally oriented and lineation is in this plane in E-W direction.

**Table 2** Summary of grain boundary orientation analysis

	Boundary type	% of length			Eigenvalue ratio		
		xz	xy	yz	xz	xy	yz
JK1B	cpx-cpx	60.95	67.13	46.60	2.12	1.88	1.20
	cpx-grt	21.09	12.58	17.84	1.29	1.31	1.05
	cpx-ru	7.59	9.32	5.31	2.20	1.53	1.29
	amp-cpx	0.34	3.61	5.49	1.18	1.60	1.31
	grt-grt	3.08	1.02	4.90	1.52	1.65	1.07
	all	x	x	x	1.76	1.69	1.12
SNW3	cpx-cpx	27.92	24.53	23.44	1.17	1.06	1.16
	cpx-grt	68.33	65.87	73.04	1.36	1.02	1.28
	grt-grt	3.75	9.60	3.52	1.10	1.38	1.13
	all	x	x	x	1.30	1.05	1.22

Percentage of important grain boundary types, eigenvalue ratios of boundary types and of all traced boundaries in sections parallel to XZ, YZ and XY planes of finite strain ellipsoid.

cpx - clinopyroxene, grt - garnet, amp - amphibole.

## 2.2 Coarse-grained eclogite (SNW3)

The sample of coarse-grained eclogite comes from the Newlands kimberlite pipe in South Africa and belongs to mantle xenoliths that were brought to the surface by kimberlite eruptions. The temperature of equilibration was estimated at 1060° - 1100°C (Gurney and Menzies, 1998). The eclogite is coarse-grained with an equilibrated microstructure, well developed macroscopic foliation and consists of slightly elongated garnet and clinopyroxene grains (Fig. II.1b). Clinopyroxene represents 56 % of volume fraction of the rock and the grain size ranges between 0.067 mm and 10.80 mm with a mean Feret diameter of 1.31 mm. Garnet represents 44 % of volume fraction of the rock and grain size ranges between 0.002 mm and 7.89 mm with a mean Feret diameter of 2.20 mm. The mean axial ratio of clinopyroxene and garnet ranges from 1.75 in XY section to 1.96 in XZ section and from 1.80 in YZ section to 2.05 in XZ section, respectively (Table II.1). The distribution of grain boundaries suggests plain strain fabric with weak preferred orientation in XZ and YZ sections with eigenvalue ratios 1.29 and 1.22, respectively, and almost no preferred orientation in XY section (eigenvalue ratio of 1.05). The grain boundary fabric is parallel to macroscopic foliation in this sample.

## 3 Lattice preferred orientation

Lattice-preferred orientation (LPO) was measured on a FEG scanning electron microscope (LEO Gemini 1530) by electron backscatter diffraction (EBSD) technique (e.g. Lloyd et al., 1991). This technique is based on automatic analysis of electron backscattered diffraction patterns (EBSP) generated by interaction of a vertical incident electron beam with a flat crystal surface tilted to 70° from the horizontal. The EBSPs are recorded online with a phosphorus screen attached to a low-light CCD camera. At each point the complete orientation of the crystal is determined. EBSPs were acquired at an accelerating voltage of 20 keV and a working distance of about 22 mm with a beam current of about 4 nA. EBSD patterns were processed and indexed using the

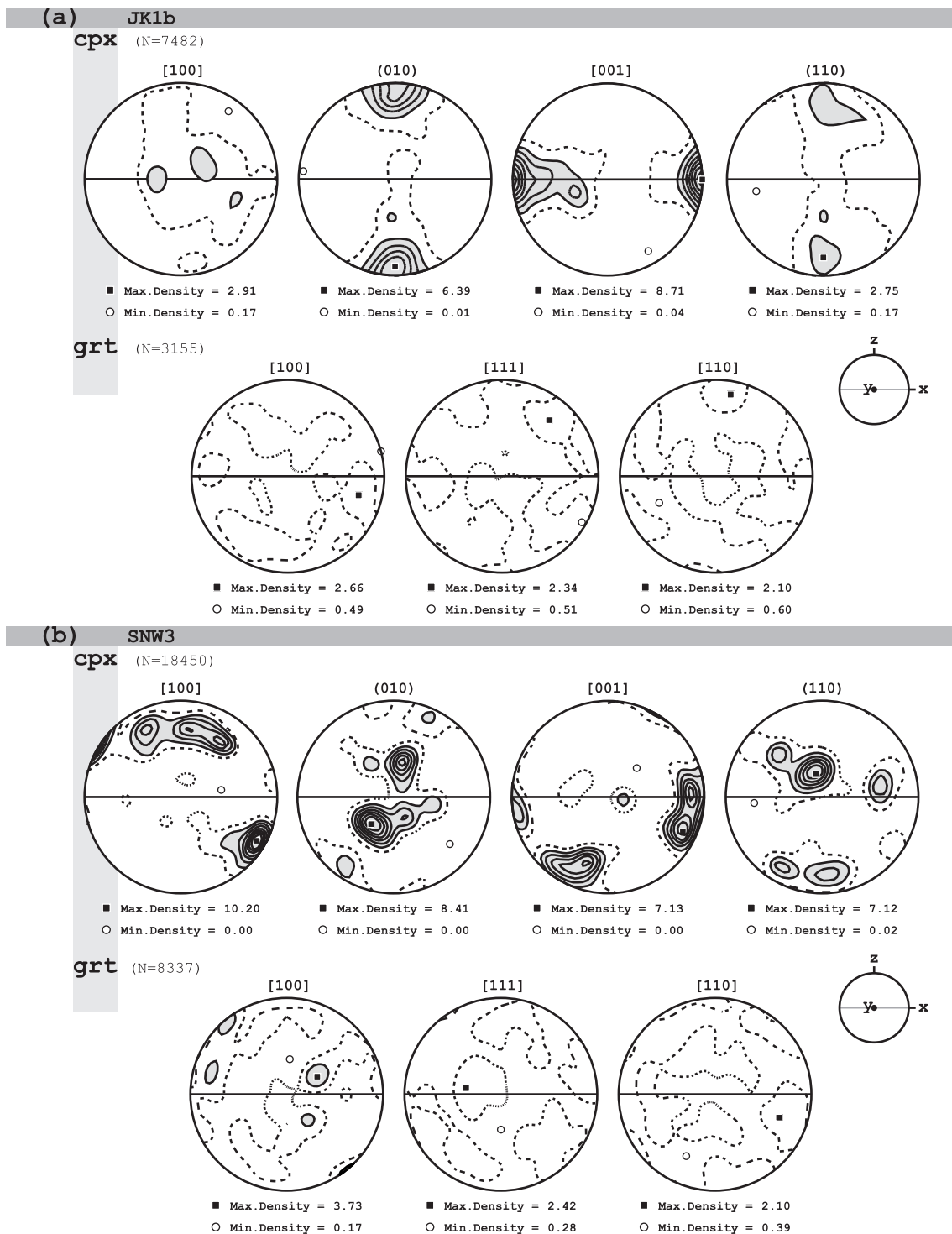


**Figure 3.** Clinopyroxene and garnet LPO of sample JK1b (a) and SNW3 (b) measured using the EBSD technique. Equal area projection, lower hemisphere. Contoured at interval 1.0 times of uniform distribution. Foliation (full line) is horizontal and lineation is in this plane in E-W direction. Number of points for each set of pole figures is noted as N.

CHANNEL5 software system by HKL Technology (Schmidt and Olesen, 1989). In sample JK1b an area of 1.5 by 1.5 mm<sup>2</sup> was measured with a step size of 10 μm. Due to the large grain size in sample SNW3 two areas of 745 and 600 mm<sup>2</sup> were measured with a step size of 250 and 200 μm respectively. The large difference in measured areas and step sizes takes into account the largely different grain sizes in the two samples so that the actual number of grains measured in each sample are about equal. For both samples thin sections oriented parallel to the XZ plane of the finite strain ellipsoid were used for the texture measurements (Fig. 3).

### 3.1 Fine-grained eclogite (JK1b)

The LPO of clinopyroxene is characterized by a strong concentration of (010)-poles perpendicular to the foliation plane and by strong concentration of [001]-axes in the foliation and parallel to the lineation (Fig. II.3a). [100]-axes are weakly concentrated close to Y axis of finite strain ellipsoid. Poles to (110) cleavage planes of clinopyroxene are concentrated in the girdle normal to lineation and foliation having two main maxima, both oriented about 60° oblique to the foliation plane. The LPO of garnet shows generally very weak density of principal crystallographic directions [100], [110] and [111]. Values of maximum density do not exceed 3 multiples of uniform distribution in any pole figure and values of minimum density are relatively high (Fig. II.3a). These results together with idiomorphic shapes of grains suggest that garnets have no LPO.

### 3.2 Coarse-grained eclogite (SNW3)

The LPO of clinopyroxene is characterized by a concentration of (010)-poles forming a girdle inclined 70° relative to the foliation plane with clearly defined maximum close to the Y-axis of finite strain ellipsoid (Fig. II.3b). [001]-axes form one maximum close to the lineation and another one which is inclined 70° to the foliation plane. The maximum density of [100]-axes is inclined 30° from the lineation in the XZ plane. A second maximum of [100]-axes is elongated and occurs oblique to the foliation plane. Poles to (110) cleavage planes show strong maximum inclined 15° from the centre of the pole figure and several weaker maxima. Such LPO with second point maximum of [001] axes located oblique to foliation plane at the margin of the pole figure does not belong to any known LPO type of clinopyroxene. The LPO of garnet in this sample is similarly weak as that in the sample JK1b. The strongest density (3.73) occurs in the pole figure of [100]-axes due to the lowest multiplicity in the crystal structure compared to [110] and [111], which is in agreement in the number of submaxima observed in all three pole figures (Fig. II.3b). The observed weak lattice preferred orientation of garnet is in agreement with the large number of slip systems available in the garnet cubic structure (Mainprice et al., 2004).

## 4 Anisotropy of P-wave velocities

P-wave velocity measurements have been carried out by means of the pulse transmission technique using the apparatus designed by Z. Pros for the measurement of spherical samples (Pros and Babuška, 1968; Pros et al. 1998). The technique allows the measurement of P-wave velocity ( $V_P$ ) in any selected direction (except for the area near the vertical axis of rotation) with the same accuracy. Here, the measurements were performed on a net dividing the sphere in steps of 15° defining 132 independent directions.

The measurement of P-wave velocity starts at atmospheric pressure and continues at several levels of confining pressure (commonly 10, 20, 50, 100, 200, 400 MPa) during increase and decrease of confining pressure. To describe the anisotropy of P-wave velocities we calculated the coefficient of anisotropy  $k$  defined as  $k = [(V_{Pmax} - V_{Pmin}) / ((V_{Pmax} + V_{Pmin})/2)] \times 100\%$ , after Birch (1961). Three sources of possible errors of measurements are considered: sample distortion, wave-picking inaccuracies and pressure instabilities. The sample distortion is mainly due to pressure induced the closing of micropores. Since we are dealing with low-porosity rocks, we estimate the resulting error of  $V_P$  at less than 1%. The wave-picking inaccuracies can be large under low confining pressure in low velocity directions and the estimated errors of  $V_P$  are around 1%. The wave-picking inaccuracies decrease rapidly with increasing confining pressure and for pressures 20-400 MPa we estimate the errors due to wave-picking inaccuracies to about 0.3-0.5%. In spite of manual corrections, the pressure instabilities during the single run of multidimensional measurements can be as high as 1 MPa (usually 0.2-0.4 MPa). We estimate the maximum errors of  $V_P$  resulting from pressure instabilities during individual runs of 3-D measurement to 1.5% for atmospheric pressure and 0.2% for maximum confining pressure.

#### **4.1 Fine-grained eclogite (JK1b)**

At minimum confining pressure (0.1 MPa), directions of high velocities form a wide belt parallel to macroscopic foliation and a broad maximum deviated by 20° from lineation direction in the foliation plane. Directions of low velocities form two strong maxima inclined about 25° to the pole of foliation (Fig. II.4a). The third maximum of low velocities is weaker and located close to lineation. At maximum confining pressure of 400 MPa, the directions of high velocities form an incomplete girdle along foliation with the maximum in the lineation, whereas the velocity minimum is perpendicular to foliation (Fig. II.4a). The spatial distribution of P-wave velocities progressively changes with increasing confining pressure with the main change between 50 MPa and 100 MPa (Fig. II.4a). Nearly the same change can be observed during decreasing pressure between 100 MPa and 50 MPa (Fig. II.4a). Maximum and minimum velocities at the highest confining pressure of 400 MPa are 8.1 kms-1 and 7.7 kms-1, respectively. The coefficient of anisotropy  $k$  is 22.4 % at 0.1 MPa and decreases with increasing confining pressure to 5.1 % at 400 MPa.

#### **4.2 Coarse-grained eclogite (SNW3)**

At minimum confining pressure, directions of both high and low velocities form broad maxima around 20° out of lineation and normal to foliation, respectively. There is no visible change in position of directions of maximum and minimum velocities with increasing confining pressure. The coefficient of anisotropy  $k$  at 0.1 MPa is 5.6 % and slightly decreases to 5.4 % at 400 MPa, maximum and minimum velocities at the highest pressure are 8.4 kms-1 and 8.0 kms-1, respectively (Fig. II.4b).

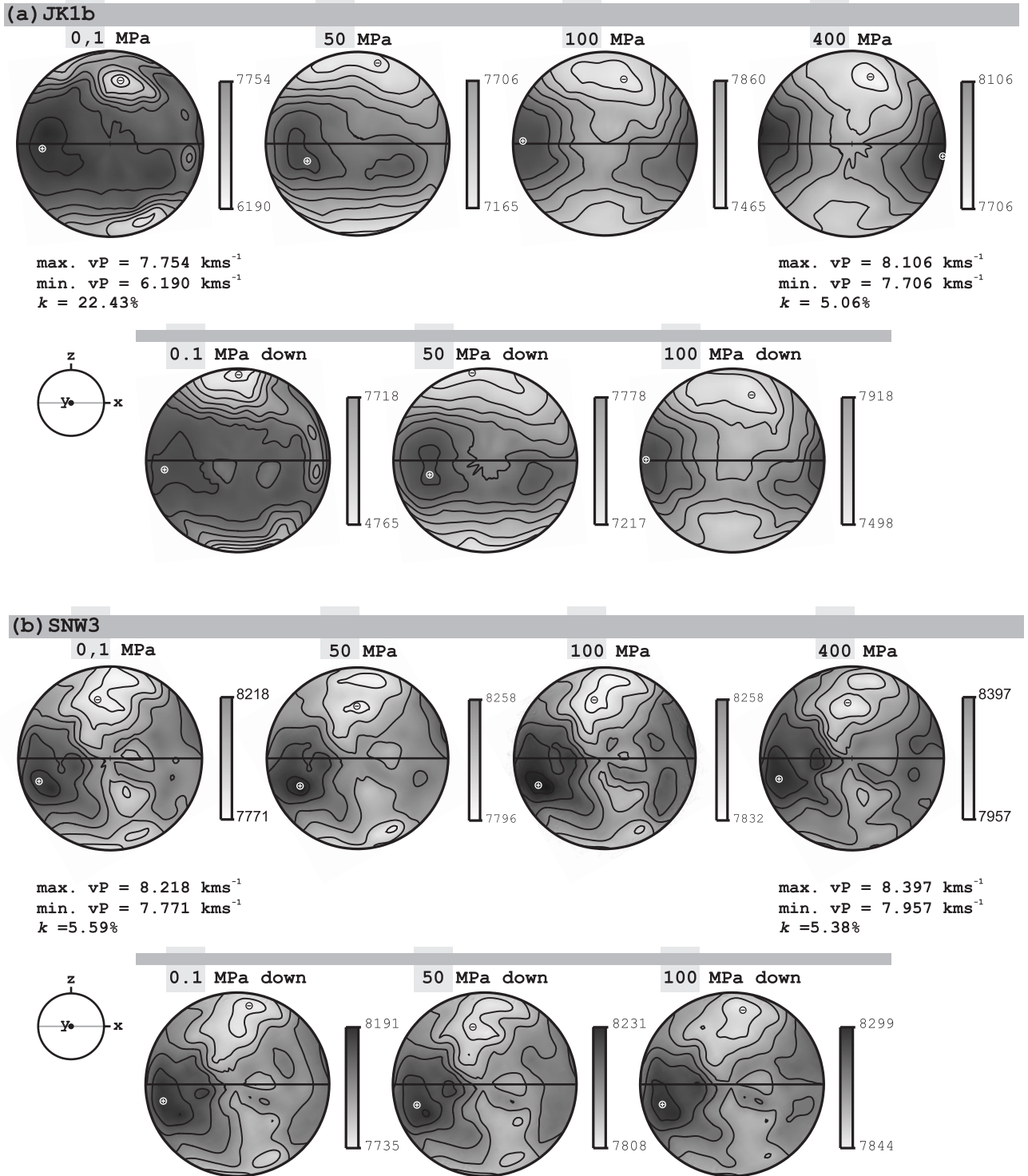


**Figure 4.** Results of measurements of P-wave velocity spatial distribution in sample JK1b (a) and sample SNW3 (b) at pressure levels 0.1, 50, 100, 400 MPa for increasing and decreasing pressure path. Diagrams are in the form of velocity isolines projected onto the lower hemisphere, equal area projection. The directions of maximum and minimum of P-wave velocities are noted by signs plus and minus. Foliation (full line) is horizontal and lineation is in this plane in E-W direction.

## 5 Orientation of microporosity

The spatial distribution of micropores has been investigated with the 3D analysis of differences between P-wave velocities measured at various confining pressures, i.e. describing the  $\Delta V_P$  ( $\Delta p$ ) dependence in space. We suppose that the change of P-wave velocity is proportional to the volume of open space that was closed between given levels of confining pressure. The  $\Delta V_P$  ( $\Delta p$ ) dependence has been studied for each pair of subsequent sets of 3D measurements in order to evaluate progressive closure of individual sets of microporosity. Examples are shown in Fig. 5, together with bulk difference of VP between 0.1 and 400 MPa. To compare the degree of preferred orientation of microporosity in the studied rocks the anisotropy of P-wave velocity difference between confining pressures of 400-0.1MPa, 400-100MPa and 100-0.1MPa were calculated as  $a = (\Delta V_{Pmax} - \Delta V_{Pmin}) / V_{Pmax}$ , where  $\Delta V_{Pmax}$  and  $\Delta V_{Pmin}$  are maximum and minimum of difference between P-wave velocities measured at given levels of confining pressure and  $V_{Pmax}$  is P-wave velocity maximum obtained at higher confining pressure. For additional description of the samples the mean of P-wave velocity differences between given pressure steps in all 132 measured directions were calculated. The mean of  $\Delta V_P$  was calculated to assign the relative amount of open space in the studied rock samples.

### 5.1 Fine-grained eclogite (JK1b)

The bulk  $\Delta V_P$  between 400 and 0.1 MPa shows a pattern which is virtually an inverse to  $V_P$  distribution at 0.1 MPa (Fig. 4a). Two main maxima (areas A and B in Fig. II.5a) are located approximately  $20^\circ$  out of the normal to foliation plane, and another, subsidiary maximum of  $\Delta V_P$  is oriented close to the direction of lineation (area C) (Fig. II.5a). In the  $\Delta V_P$  diagram for 10-0.1 MPa, two maxima corresponding to areas A and B are visible. For the pressure level of 20-10 MPa, the  $\Delta V_P$  diagram shows a combination of the areas A and B forming single maximum. Between 50 and 20 MPa, a strong maximum of P-wave velocity differences is located in area B. Other two submaxima are oriented close to a direction of lineation (near area C). The values of maxima in partial  $\Delta V_P$  diagrams are decreasing with increasing confining pressure from  $0.8 \text{ kms}^{-1}$  to  $0.3 \text{ kms}^{-1}$ . The anisotropy of  $V_P$  difference between 400 and 0.1 MPa is 15.5 % and the mean  $\Delta V_P$  is  $0.6 \text{ km}^{-1}$ . Partial  $\Delta V_P$  diagrams indicate that most microporosity of the set corresponding to the area A closed down between 0.1 and 20 MPa. Most microporosity corresponding to the area B and C closed between 0.1 and 50MPa (Fig. 5a).

### 5.2 Coarse-grained eclogite (SNW3)

In the sample SNW3, the bulk  $\Delta V_P$  between 400 and 0.1 MPa shows three approximately orthogonally located maxima: the first normal to foliation plane, the second about  $30^\circ$  from the centre of the diagram in the foliation plane and the third about  $30^\circ$  from the lineation direction in the foliation plane (Fig. II.5b). All partial  $\Delta V_P$  diagrams show neither strong individual maxima or minima nor progressive lowering of absolute maximum value of  $\Delta V_P$  within the individual pressure levels (Fig. II.5b). There are several partial maxima and minima in  $\Delta V_P$  diagram, whose position changes with pressure, and surprisingly, the absolute values of maximum  $\Delta V_P$  slightly increase with increasing confining pressure. However, all these values are close to the estimated value of error of experimental measurement. The  $V_P$  difference anisotropy between 400 and 0.1MPa is 3.0 % and the mean  $\Delta V_P$  is  $0.2 \text{ kms}^{-1}$ .

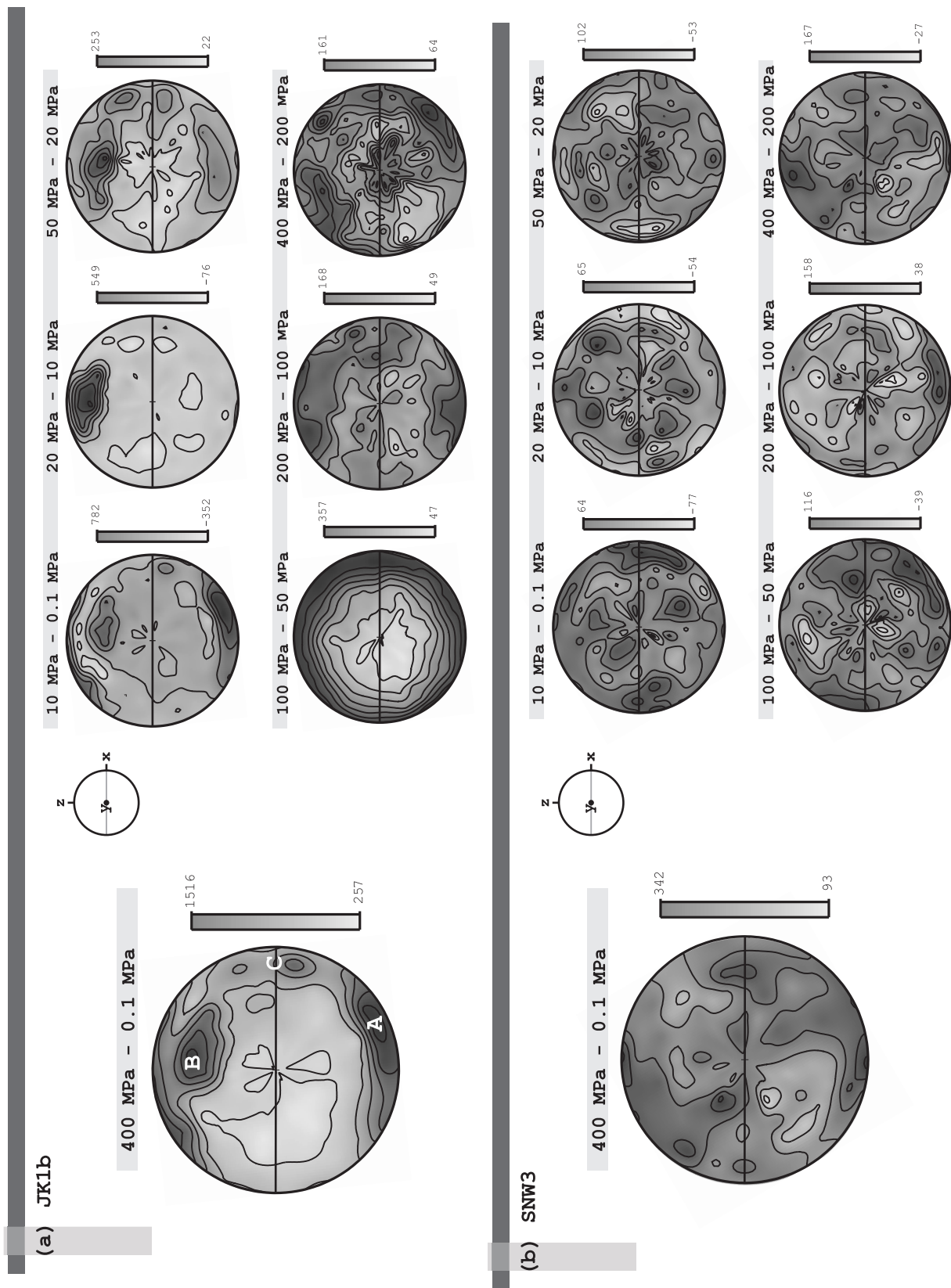


**Figure 5.** Stereodiagrams of the  $\Delta V_p(\Delta p)$  dependence in space for samples JK1b (a) and SNW3 (b). It shows diagrams of each pair of subsequent sets of 3D measurements together with bulk difference of  $V_p$  between 0.1 and 400 MPa. Orientation of foliation and lineation is same as in figure II.4.

## 6 Discussion

The spatial distribution of P-wave velocities at 400 MPa is more or less similar in both samples and corresponds well to the observed lattice preferred orientation (LPO) of clinopyroxene (Figs. II.3 and II.4). The LPO of clinopyroxene in the fine-grained sample JK1b is characterized by a strong concentration of c-axes [001] in the direction of stretching lineation. The direction of high P-wave velocities is also oriented close to the lineation, which can be correlated to the single crystal model of P-wave velocities in clinopyroxene. The more diffuse orientation of directions of high P-wave velocities and the oblique orientation of the maximum velocity with respect to foliation in the sample SNW3 can be probably explained by the presence of clinopyroxene c-axes sub-maxima declining  $70^\circ$  from the foliation plane. In spite of the abundance of garnet, it does not influence the directional dependence of velocity due to its high symmetry and low elastic anisotropy (e.g. Babuška et al., 1978). In both samples, the P-wave velocity and its anisotropy are in the range of observations in eclogites from other orogens (Fountain et al., 1994; Kumazawa et al., 1971; Mauler et al., 2000). However, the presence of about 13% of randomly oriented mineral phases with lower P-wave velocity as amphibole, quartz, paragonite and zoisite are very likely the main reason for the lower measured velocities.

The evolution of the spatial distribution of P-wave velocities with increasing pressure is different in both samples. In the coarse-grained sample SNW3, the spatial distribution of P-wave velocities at 0.1 MPa is similar to that observed at 400 MPa. The maximum and minimum velocities ( $8.2 \text{ km s}^{-1}$  and  $7.8 \text{ km s}^{-1}$ , respectively) are only slightly lower compared to the values obtained at maximum pressure conditions. Also, the degree of anisotropy shows only a very small difference between maximum and minimum pressure conditions (Fig. II.4b). On the contrary, the differences between the velocities obtained at 400 and 0.1 MPa are much more significant in the fine grained sample. The major change of spatial distribution of the P-wave velocities takes place between 50 and 100 MPa as can be seen in the differential diagram in Fig. II.5a. The difference between the spatial distribution of P-wave velocities in the sample JK1b obtained at maximum and minimum confining pressure is likely caused by preferentially oriented microporosity. The important effect of microporosity on P-wave velocities and their spatial distribution at low confining pressures is indicated by high degree of anisotropy ( $k = 22.4 \%$ ) and low values of maximum and minimum velocity measured at atmospheric pressure ( $7.8 \text{ km s}^{-1}$  and  $6.2 \text{ km s}^{-1}$ , respectively).

In the sample JK1b, the microporosity is preferentially oriented in two main directions, denoted as areas A and B in Fig. II.5a. Individual differential diagrams show that the pores corresponding to the area A are closed at lower pressures (20 MPa) than the pores corresponding to the area B, whilst the majority of pores are closed above 50 MPa. This indicates the presence of several types of microporosity with different response to confining pressure (cf. Babuška and Pros, 1984; Siegesmund and Vollbrecht, 1991). The most probable microscopic features responsible for oriented microporosity in this sample are grain boundaries and cleavage planes in clinopyroxene. There are other minerals having cleavage planes in the sample, but they are much less abundant than clinopyroxene and they are not preferentially oriented. The quantitative microstructural analysis shows a strong constrictional fabric of grain boundaries with the largest population oriented subparallel to the foliation plane (Fig. II.2a.b). Lattice preferred orientation shows the (110) cleavage planes concentrated in the girdle normal to lineation having two maxima, both oriented about  $60^\circ$  from the foliation plane

(Fig. II.3a). These data suggest that the area A in Fig. II.5a may correspond to grain boundaries parallel to foliation plane and the area B most likely corresponds to the cleavage planes. In this sample, the grain boundaries were therefore closed prior to the cleavage planes as a result of increasing confining pressure.

In the second sample, SNW3, the microporosity forms three orthogonally oriented maxima as seen in the differential diagram in Fig. II.5b. Nevertheless, no systematic evolution of microporosity orientation with increasing pressure was observed. The quantitative microstructural analysis of the sample SNW3 shows a weak plane strain fabric of grain boundaries, with the strongest preferred orientation parallel to the foliation plane (Fig. II.2c,d). The determined preferred orientation of cleavage planes (110) in clinopyroxene shows a strong maximum inclined  $15^\circ$  away from the Y-axis of strain ellipsoid and two other weaker maxima (Fig. II.3b). All three maxima correspond well with the orientation of maxima in the differential diagrams of  $V_p$ . This seems to indicate that the open space along the cleavage planes in clinopyroxene represents a major part of the microporosity and the grain boundaries contribute to the bulk porosity only in the direction perpendicular to the foliation plane.

The mean and the anisotropy of P-wave velocity differences were calculated to assign the relative amount of microporosity and the degree of its preferred orientation. The mean P-wave velocity difference is  $0.6 \text{ kms}^{-1}$  in the fine-grained sample JK1b and  $0.2 \text{ kms}^{-1}$  in the coarse-grained sample SNW3. The anisotropy of bulk microporosity reached 15.5% in fine-grained sample JK1b and 2.9% in coarse-grained sample SNW3. These data suggest that in the sample JK1b the microporosity is relatively large and strongly preferentially oriented, in contrast to the sample SNW3 in which it is significantly lower and weakly oriented. This is in agreement with the assumption that the grain boundaries are the most important carriers of microporosity in eclogites. The orientation of microporosity thus seems to depend mostly on the preferred orientation of grain boundaries and rather less on the orientation of (110) cleavage planes in clinopyroxene.

We assume that micropores which are preferentially oriented parallel to grain boundaries (grain boundary porosity) have a shape of planar cracks in our samples, since their closing at higher pressures leads to a change (decrease) of velocity anisotropy. It is very likely that the micropores parallel to the (110) clinopyroxene cleavage planes also have the shape of planar cracks. So we suggest that grain-boundary cracks and cleavage cracks parallel to the (110) clinopyroxene planes are responsible for the main part of microporosity. Such microcracks and corresponding porosity have been most probably formed during exhumation process, as an inelastic response to the decrease of lithostatic stress and an elastic mismatch between grains.

## 7 Conclusions

Using a combination of three independent research methods - microstructural analysis, measurement of lattice preferred orientation and 3-D measurement of elastic P-wave velocity - we were able to document the pressure-dependent behavior and distinguish the differences of two main anticipated carriers of microporosity in two samples of eclogite - crystal cleavage and grain boundaries.

The following main observations were made:

1. Microporosity in fine-grained and coarse-grained eclogites is related to grain boundaries and cleavage planes in clinopyroxene.

2. In the fine-grained sample, the microporosity is relatively large and strongly preferentially oriented. The grain boundaries oriented parallel to the foliation plane contribute mainly to the bulk microporosity.

3. In the coarse-grained sample, microporosity is relatively low and weakly preferentially oriented. The cleavage planes in clinopyroxene are responsible for the main part of preferentially oriented microporosity.

4. The grain boundaries have much stronger influence on orientation and amount of microporosity than the cleavage planes in both samples.

5. With increasing confining pressure, grain boundaries close below 50 MPa, while cleavage planes in clinopyroxene remain open up to 100 MPa. Orientation of microporosity mostly depends on preferred orientation of grain boundaries and somewhat less on orientation of cleavage planes in clinopyroxene. We conclude that grain-boundary cracks and cleavage cracks parallel to clinopyroxene (110) planes are responsible for the main part of microporosity.

## Acknowledgements

We would like thank to V. Babuška for critical comments on the manuscript. We also thank to two anonymous reviewers and the editor for their useful comments. This work was supported by grants of Czech National Grant Agency No. 205/03/P065 to S. Ulrich and from resources of Research Intent to Geophysical Institute of the Academy of Sciences of the Czech Republic No. AV0Z30120515. The research was also partly supported by GACR, and Czech Ministry of Education through research projects no. 205/02/D139 and MSM 0021622412.

## References

- Åkesson, U., J. Hansson, and J. Stigh (2004), Characterisation of microcracks in the Bohus granite, western Sweden, caused by uniaxial cyclic loading, *Engineering Geology*, 72 (1-2), 131-142, doi:10.1016/j.enggeo. 2003.07.001.
- Babuška, V., and Z. Pros (1977), Effect of fabric and cracks on the elastic anisotropy in granodiorite, *Inst. Geophys. Pol. Acad. Sci.*, A-6,(117), 179- 186.
- Babuška, V., and Z. Pros (1984), Velocity anisotropy in granodiorite and quartzite due to the distribution of microcracks, *Geophysical Journal of The Royal Astronomical Society*, 76 (1), 121.
- Babuška, V., J. Fiala, M. Kumazawa, I. Ohno, and Y. Sumino (1978), Elastic properties of garnet solid-solution series, *Physics of The Earth and Planetary Interiors*, 16 (2), 157-176.
- Birch, F. (1961), Velocity of compressional waves in rocks to 10 kilobars, .2., *Journal of Geophysical Research*, 66 (7), 2199-2224.
- Brace, W. (1965), Relation of elastic properties of rocks to fabric, *Journal of Geophysical Research*, 70 (22), 5657-5667.
- Fountain, D., T. Boundy, H. Austrheim, and P. Rey (1994), Eclogite-facies shear zones deep crustal reflectors? *Tectonophysics*, 232 (1-4), 411-424.

- Gurney, J. J., and A. Menzies (1998), The Newlands kimberlite pipes and dyke complex, in *Small Mines Field Excursion guide*, 7th International Kimberlite Conference. Cape Town, South Africa, vol. , pp. 23-30.
- Kanaori, Y., K. Yairi, and T. Ishida (1991), Grain-boundary microcracking of granite rocks from the northeastern region of the Atotsugawa fault, Central Japan - SEM backscattered electron images, *Engineering Geology*, 30 (2), 221- 235.
- Klápová, H., J. Konopásek, and K. Schulmann (1998), Eclogites from the Czech part of the Erzgebirge: multi-stage metamorphic and structural evolution, *Journal of The Geological Society*, 155 (Part 3), 567-583.
- Kumazawa, M., H. Helmstaedt, and K. Masaki (1971), Elastic properties of eclogite xenoliths from diatremes of East Colorado plateau and their implication to upper mantle structure, *Journal of Geophysical Research*, 76 (5), 1231-1247.
- Lexa, O., P. Štípska, K. Schulmann, L. Baratoux, and A. Kroner (2005), Contrasting textural record of two distinct metamorphic events of similar P-T conditions and different durations, *Journal of Metamorphic Geology*, 23 (8), 649-666, doi:10.1111/j.1525-1314.2005.00601.x.
- Lloyd, G., N. Schmidt, D. Mainprice, and D. Prior (1991), Crystallographic textures, *Mineralogical Magazine*, 55 (380), 331-345.
- Mainprice, D., Bascou, J., Cordier, P., Tommasi, A. (2004), Crystal preferred orientations of garnet: comparison between numerical simulations and electron backscattered diffraction (EBSD) measurements in naturally deformed eclogites, *Journal of Structural Geology*, 26 (11), 2089–2102.
- Mauler, A., L. Burlini, K. Kunze, P. Philippot, and J. Burg (2000), P-wave anisotropy in eclogites and relationship to the omphacite crystallographic fabric, *Physics and Chemistry of The Earth Part A-Solid Earth and Geodesy*, 25 (2), 119-126.
- Menendez, B., C. David, and A. Nistal (2001), Confocal scanning laser microscopy applied to the study of pore and crack networks in rocks, *Computers & Geosciences*, 27 (9), 1101-1109.
- Pros, Z., and V. Babuška (1968), An apparatus for investigating elastic anisotropy on spherical rock samples, *Studia Geophysica et Geodaetica*, 12 (2), 192-198.
- Pros, Z., T. Lokajíček, and K. Klíma (1998), Laboratory approach to the study of elastic anisotropy on rock samples, *Pure and Applied Geophysics*, 151 (2-4), 619-629.
- Schild, M., S. Siegesmund, A. Vollbrecht, and M. Mazurek (2001), Characterization of granite matrix porosity and pore-space geometry by in situ and laboratory methods, *Geophysical Journal International*, 146 (1), 111-125.
- Schmidt, N., and N. Olesen (1989), Computer-aided determination of crystallattice orientation from electron-channeling patterns in the SEM, *Canadian Mineralogist*, 27 (Part 1), 15-22.
- Siegesmund, S., and A. Vollbrecht (1991), Complete seismic properties obtained from microcrack fabrics and textures in an amphibolite from the ivrea zone, western alps, italy, *Tectonophysics*, 199 (1), 13-24.

- Siegesmund, S., A. Vollbrecht, and G. Nover (1991), Anisotropy of compressional wave velocities, complex electrical-resistivity and magnetic-susceptibility of mylonites from the deeper crust and their relation to the rock fabric, *Earth and Planetary Science Letters*, 105 (1-3), 247-259.
- Siegesmund, S., A. Vollbrecht, and Z. Pros (1993), Fabric changes and their influence on p-wave velocity patterns - examples from a polyphase deformed orthogneiss, *Tectonophysics*, 225 (4), 477-492. 8
- Takeshita, T., and K. Yagi (2001), Paleostress orientation from 3-D orientation distribution of microcracks in quartz from the Cretaceous granodiorite core samples drilled through the Nojima Fault, south-west Japan, *Island Arc*, 10 (3- 4), 495-505.